

## Structure–activity relationship of a peptide permeation enhancer

Joël Brunner and Gerrit Borchard

Section of Pharmaceutical Sciences, Institute of Pharmaceutical Sciences of Western Switzerland (ISPSO), University of Geneva, Switzerland

### ABSTRACT

The pentapeptide L-R5 has previously been shown to transiently increase the permeability of nasal epithelial cell layers *in vitro*, allowing paracellular transport of molecules of up to 4 kDa. Protein kinase C zeta (PKC  $\zeta$ ), a member of a family of serine/threonine kinases was shown to be involved in tight junction modulation induced by L-R5. We show here that the ability of L-R5 to modulate tight junctions is comparable to other permeability enhancers such as bilobalide, latrunculin A or C<sub>10</sub>. Interaction of the peptide with the target protein occurs via electrostatic interaction, with the presence of positive charges being essential for its functionality. L-R5 is myristoylated to allow quick cell entry and onset of activity. While no epithelial cytotoxicity was detected, the hydrophobic myristoyl rest was shown to cause haemolysis. Taken together, these data show that a structural optimization of L-R5 may be possible, both from a toxicological and an efficacy point of view.

### ARTICLE HISTORY

Received 22 February 2022  
Revised 28 March 2022  
Accepted 28 March 2022

### KEYWORDS

Epithelial permeability; tight junctions; TEER; L-R5; PKC zeta; permeation enhancer

## 1. Introduction

Drug development is often hampered by the physicochemical properties of the drug candidate. The selection of excipients may lead to an optimization of key pharmacokinetic parameters such as absorption and distribution.<sup>1</sup> Since the majority of approved drugs are administered orally,<sup>2</sup> sufficient intestinal absorption and resulting bioavailability is decisive for drug efficacy and safety. At epithelia, drug absorption can occur by the transcellular or paracellular pathway.<sup>3</sup> It has been estimated that the intercellular (paracellular) space in the intestinal epithelium is about 4 Å.<sup>4</sup> In addition, the passage of molecules through the paracellular space is regulated by networks of proteins forming different types of intercellular junctions. The most important of these connections are tight junctions (TJs),<sup>5</sup> located at the apical side of the epithelial cells.

TJs comprise a network of different proteins, with the most important being occludin,<sup>6</sup> zonula occludens proteins (ZO-1, -2)<sup>7</sup> and the claudin family.<sup>8</sup> The modulation of these junctions is a dynamic process triggered by intracellular and/or extracellular stimuli, such as inflammatory signals.<sup>9,10</sup> In addition to managing cell tissue

permeability, TJs also play a role in cell differentiation and proliferation, as well as in the establishment of cell polarity.<sup>11,12</sup> In addition, TJs also close the intercellular space between the apical and basolateral sides, and form a transmembrane exchange zone (TJ fence function).<sup>13</sup> Their regulation is mainly regulated by protein kinases C (PKCs).<sup>14,15</sup> The controlled modification of these junctions has been one of the pathways used to open the intercellular space, thereby increasing paracellular permeability.

In order to increase oral bioavailability of drugs, different types of permeation enhancers (PEs) have been developed<sup>16</sup> that act through different mechanisms of TJ modulation, but also of other types of intercellular connections such as adherens junctions (AJs). Modulation of these junctions in a selective manner would allow to transiently increase transepithelial permeability. Several PEs have been introduced into the market, such as SNAC and C<sub>10</sub>.<sup>17</sup> Some of these PEs have a well-described mechanism of action, such as bilobalide, which interacts with the adenosine A1 receptor,<sup>18</sup> or latrunculin A, which interferes with the cytoskeleton structure.<sup>19</sup> An issue to be addressed is the potential toxicity of these PEs, as has been described, for example, for sodium dodecyl sulfate

(SDS).<sup>20</sup> PEs addressing the regulation of TJ proteins such as occludin and ZO-1<sup>21,22</sup> may directly lead to an increase in epithelial permeability through a well-defined mechanism. Accordingly, PKCs, which regulate the balance of certain TJ proteins are prime targets for such a PE.

PKCs are a family of serine/threonine kinases.<sup>23</sup> These enzymes have been identified to be involved in many intracellular mechanisms, such as apoptosis,<sup>24</sup> proliferation,<sup>25</sup> or inflammation,<sup>26</sup> and are grouped into conventional, novel, and atypical PKC subfamilies.<sup>27</sup> PKCs may have opposing roles.<sup>16</sup> An imbalance in their expression was found in certain diseases, such as certain cancer types, where an increase in the expression of certain PKCs is present,<sup>28</sup> and in diabetes.<sup>29</sup> Management of this expression imbalance through therapeutic intervention has already been studied, however, until now in the absence of real clinical success.<sup>30</sup>

PKC  $\zeta$  belongs to the atypical sub-family and has been identified to be overexpressed in some cancer types.<sup>31</sup> In addition, this kinase has also been found to be responsible for the activation of the TJ proteins occludin<sup>32</sup> and ZO-1<sup>33</sup> through phosphorylation of threonine and serine residues, respectively. Phosphorylation takes place through the interaction between PKC  $\zeta$  and the target proteins mediated by the pseudosubstrate (PS) part of the enzyme through electrostatic interaction<sup>34</sup> (Figure 1). The PS is a segment that is part of the enzyme between the amino acids 113 and 129<sup>35</sup> and has initially a self-inhibitory function on the enzyme keeping it in an inactive state.<sup>36</sup> When PKC  $\zeta$  is activated, the role of

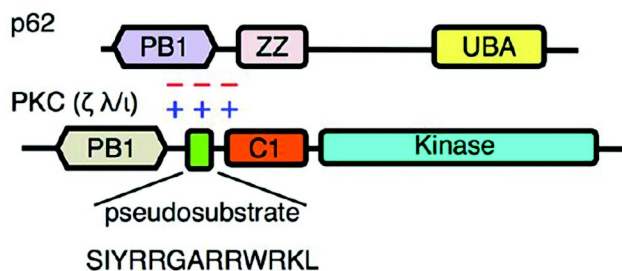


**Figure 1.** Mechanism of electrostatic interaction between PS of PKC  $\zeta$  and the target protein (here p62). In a normal situation PS interacts with a part of the target protein (here PB1). The zeta inhibitory peptide (ZIP) competes with the PS and prevents interaction between the enzyme and the protein. Phosphorylation and activation of the target protein does not occur.<sup>34</sup>

the PS is to interact with the target protein to allow its phosphorylation.<sup>34</sup> Inhibition of PKC  $\zeta$  may prevent the activation of TJ proteins and the closure of these junctions, increasing paracellular permeability.

A myristoylated peptide with the PS sequence of PKC  $\zeta$  (zeta inhibitory peptide ZIP) has been commercialized as an inhibitor of the enzyme.<sup>37</sup> Inhibition of the kinase by ZIP was originally thought to be achieved by taking the place of the PS to keep PKC  $\zeta$  in an inactive state. However, it was recently shown<sup>34</sup> that this peptide does not interact with the enzyme. A ZIP-derived peptide (L-R5) tested in our laboratory showed that the inhibition of PKC  $\zeta$  activity was not achieved by interacting with the enzyme, but with the target protein.<sup>38</sup> The interaction between PS and occludin, for example, was competitively blocked by the presence of L-R5, inhibiting phosphorylation and thus activation of TJ proteins. Moreover, a decrease of TJ proteins expression by ZIP has been noted.<sup>38,39</sup>

The increase in permeability by L-R5 entering in the cell has already been demonstrated,<sup>40</sup> as has its lack of epithelial cytotoxicity *in vitro*. This study further characterizes L-R5, compares the peptide to other PEs, and assesses the toxicity of several fatty acids potentially replacing the myristoyl rest toward an improved efficacy of the peptide.

## 2. Materials and methods

### 2.1. Materials

Phosphate buffered saline (PBS) solution, sodium pyruvate, Dulbecco's Modified Eagle's Medium (DMEM), penicillin and streptomycin (penstrep), non-essential amino acids (NEAA), foetal bovine serum (FBS), Hank's balanced saline solution (HBSS), trypsin EDTA and saline solution (NaCl 0.9%) were obtained from Gibco (Zug, Switzerland). Latrunculin A, bilobalide, sodium caprate (C<sub>10</sub>) (Table 1), collagen solution PureCol, myristoyl-Gly (myr), methyl myristoleate (myro), methyl octanoate (octa) and methyl palmitate (palm) were obtained from Sigma-Aldrich (Buchs, Switzerland). Sodium fluorescein, fluorescein dextran 4 kDa, fluorescein dextran 150 kDa and fresh defibrinated sheep blood were obtained from Thermo Fisher Scientific (Zug, Switzerland). Water for injection (WFI), T75 flasks,

**Table 1.** Permeation enhancers used and their suggested mechanism of action.

Permeation enhancer	Mechanism of action	Concentration reported	Reference
Latrunculin A	Prevents actin repolymerization, disrupts actin cytoskeleton	0.2 $\mu$ M	40
Bilobalide	A1R-mediated phosphorylation of actin-binding proteins	5 $\mu$ M	41
Sodium caprate	Reversible removal of tricellulin from tricellular tight junction	8.5 mM	20
Sodium dodecylsulfate	Integration into cell membrane increasing cell membrane fluidity causing loss of integrity and increase in permeability	2 mM	42

96-well plates as well as 24-well plates with 6.5 mm inserts of 0.4  $\mu$ m pore size and a surface area of 0.33 cm<sup>2</sup> were obtained from Corning (Root, Switzerland). Sodium dodecylsulfate (SDS) was purchased from Merck (Schaffhausen, Switzerland). Ethanol 99.8% was purchased from Biosolve (Dieuze, France). Caco-2 cells were purchased from ATCC (HTB-37, Manassas, USA). WST-1 reagent was purchased from Roche (Basel, Switzerland). All peptides were obtained from Bachem AG (Bubendorf, Switzerland), their respective structures are detailed in Table 2.

## 2.2. Cell culture

Mycoplasma-free Caco-2 cells were cultured in T75 flasks in a humidified atmosphere at 37°C and 5% CO<sub>2</sub>. These cells were used at passage numbers 35–39. Cells were cultured in DMEM supplemented with 10% FBS, 1% PenStrep, 1% NEAA and 1% sodium pyruvate. The medium was changed every 2 to 3 days, and the cells were passaged using trypsin every 5 days at a split ratio of 1:3. For toxicity studies, cells were seeded at a density of 4.5 × 10<sup>4</sup> cells/cm<sup>2</sup> in 96-well plates. 100  $\mu$ l of medium was added and cells were incubated for 2 days. 24-well plate inserts were coated for 3 hours with a 0.003% collagen solution in PBS before seeding cells at a density of 6 × 10<sup>4</sup> cells/cm<sup>2</sup>. 600  $\mu$ l and 100  $\mu$ l of medium were changed every 2 to 3 days on the basolateral and apical side, respectively, for 21 days. Before the start of permeability experiments, cells were equilibrated in warm HBSS with the same volumes for 30 minutes in the incubator under the conditions described above.

**Table 2.** Designation and structures of peptides used.

Peptide designation	Peptide structure
L-R5	L-myr-ARRWR
D-R5	D-myr-ARRWR
Scrambled	L-myr-WRARR
L-A5	L-myr-AARWR
L-W5	L-myr-ARRAR
ZIP	L-myr-SIYRRGARRWRKL

myr: myristoyl; ZIP: zeta inhibitory peptide

## 2.3. Assessment of cytotoxicity

Impact of the peptides and fatty acids (FA) on cell proliferation as a measure of toxicity was tested by WST-1 assay. The peptide solutions in NaCl 0.9% had concentrations between 25 and 100  $\mu$ M, and FA solutions between 50  $\mu$ M and 5 mM. SDS 0.1% in water for injection and culture medium were used as positive control and negative controls, respectively. The prepared cell plate was taken out of the incubator and 100  $\mu$ l of the different solutions were applied, mixed with culture medium, and incubated for 24 hours under conditions as described above. Finally, the supernatant was removed and a mix (100  $\mu$ l) of WST-1 reagent and cell culture medium at a ratio of 1:1 was added. Absorbance was measured at 450 nm and 690 nm after 2 hours with a plate reader (Biotek Synergy Mx, Sursee, Switzerland). The signal measured by the second wavelength was considered as the baseline. To determine the percentage of cellular viability, equation 1 was used:

$$\text{Cytotoxicity}(\%) = \frac{\text{Abs}_{\text{exp value}} - \text{Abs}_{\text{neg control}}}{\text{Abs}_{\text{pos control}} - \text{Abs}_{\text{neg control}}} \times 100 \quad (1)$$

## 2.4. In vitro haemolysis assay

As previously described,<sup>40</sup> fresh defibrinated sheep blood was used to evaluate the influence of peptides and fatty acids on the integrity of the cellular membranes. The blood was washed using PBS and centrifuged at 1500 rpm for 1 minute. Supernatant was discarded and the pellet was resuspended in 1 ml of PBS. These steps were repeated 5 times. Finally, 11 ml of PBS were added, and the suspension was stored at 4°C. Solutions of peptides and fatty acids (myr, myro, octa, palm) at concentrations between 1 mM and 5  $\mu$ M were prepared in HBSS. WFI was used as a positive control and HBSS was used as a negative control. 50  $\mu$ l of each condition were incubated with 50  $\mu$ l of washed sheep blood

suspension (47.2 million cells/ml) in each well of a round bottom 96-well plate for 30 minutes under slow agitation at room temperature. The plate was centrifuged at 3700 rpm for 10 minutes. 50  $\mu$ l of supernatant of each well was then transferred and mixed with 250  $\mu$ l of ethanol in a flat bottom 96 well plate. The absorbance was then read at 412 nm (Biotek Synergy Mx, Sursee, Switzerland) with a maximum of 0.724 and a minimum of 0.095, respectively, for WFI and HBSS. The absorbance values obtained for the positive control were defined as 100% haemolysis and the negative control as 0%.

### 2.5. Transepithelial electrical resistance

Transepithelial electrical resistance (TEER) was measured as previously described<sup>40</sup> right after the equilibration of the cells and immediately after the permeability experiments using an EVOM volt-ohmmeter (World Precision Instruments, Stevenage, UK) equipped with chopstick electrodes. TEER values were calculated by using equation 2:

$$\text{TEER } (\Omega \text{ cm}^2) = (\text{resistance value } (\Omega) - 100 (\Omega)) \times 0.33 (\text{cm}^2) \quad (2)$$

where 100 ( $\Omega$ ) is the resistance of the porous membrane coated with the collagen layer the cells were seeded upon, and 0.33  $\text{cm}^2$  is the total surface of the epithelial cell layer and of the insert. TEER was always measured in warm HBSS.

### 2.6. Permeability studies

As previously described,<sup>40</sup> the apparent permeability ( $P_{\text{app}}$ ) of fluorescein dextran 4 kDa (FD-4) and 150 kDa (FD-150) was calculated using the equation 3:

$$P_{\text{app}} = \frac{\Delta Q}{\Delta t} \times \frac{1}{A \times C_0} \quad (3)$$

where  $C_0$  is the initial concentration ( $10^6$  ng/ml) of the permeant in the donor compartment (apical side),  $A$  is the surface area of the cell layers (0.33  $\text{cm}^2$  for inserts in 24 well plates) and  $dQ/dt$  is the appearance rate of FD-4 or FD-150 in the receiver compartment (basolateral side). All experiments were performed in triplicate.

After equilibration and TEER measurement, the peptide or FA solutions containing 0.25 mM FD-4 or 6.6  $\mu$ M of FD-150 in HBSS were applied to the apical side. The concentration of the other PEs was determined based on the literature referring to their permeability enhancing effect. Instead of peptides or FA, bilobalide,<sup>41</sup> latrunculin A,<sup>42</sup> SDS<sup>43</sup> and  $C_{10}$ <sup>20</sup> were applied at a concentration of 5  $\mu$ M, 0.2  $\mu$ M, 2 mM, and 8.5 mM, respectively. Samples of 100  $\mu$ l were taken from the basolateral compartment of each well every 15 minutes during the first half hour, and then each 30 minutes for a final period of 3 hours, with each volume being replaced by an equal volume of warm HBSS to maintain sink conditions. The fluorescence of FD-4 and FD-150 was then measured in black 96-well plates at excitation and emission wavelengths of 485 and 520 nm, respectively, using a plate reader (Biotek Synergy Mx, Sursee, Switzerland). A calibration curve was established to determine the concentration of the fluorescent compound over time at the basolateral side.

### 2.7. Statistical analysis

Data are reported as mean  $\pm$  standard deviation (S. D.). Statistical significance was considered at a  $p$ -value  $< 0.05$ . Significance is denoted as \* $p < 0.05$ , \*\*  $p < 0.01$ , \*\*\*  $p < 0.001$ , \*\*\*\*  $p < 0.0001$ . The data were analyzed using two-way analysis multiple comparison of variance (ANOVA) with GraphPad Prism. The data were analyzed using multiple t-test comparisons.

## 3. Results

### 3.1. L-R5 compared to other PEs

The L-R5 peptide had already shown its ability to increase the permeability of molecules through an epithelial cell layer.<sup>40</sup> This increase in permeability and decrease in TEER was compared to other PEs with different mechanisms of action (Table 1). L-R5 was compared to bilobalide and latrunculin A (Figure 2A,B), and subsequently to  $C_{10}$  and SDS (Figure 2C,D). The passage of FD-4 is further increased by L-R5 compared to latrunculin A and bilobalide, which showed similar increases in permeability. The decrease in TEER, however, is comparable between the 3 PEs. By contrast, both SDS

and C<sub>10</sub> drastically decreased TEER at concentrations tested. Epithelial permeability caused by C<sub>10</sub> showed a strong increase only after 150 minutes, which corroborates data previously reported in the literature.<sup>17</sup> On the other hand, the effect of surface-active agent SDS is considered to be due to its toxicity.<sup>44</sup>

### 3.2. Influence of fatty acids on permeability and toxicity

The impact of length or state of saturation of the fatty acid moiety on *in vitro* cytotoxicity and permeability was examined. A haemolysis test was performed on defibrinated blood cells (Figure 3A) with fatty acids of different chain lengths (C8:0 octanoyl, C13:0 myristoyl and C16:0 palmitoyl) as well as an unsaturated myristoleyl (C13:1) moiety and L-R5, which is myristoylated. The extent of haemolysis was detected to increase with the chain length of the fatty acid. Furthermore, the unsaturated fatty acid showed a higher hemolytic index than the other fatty acids, despite being shorter

than palmitoyl. In addition to the haemolysis test, a WST-1 cell toxicity test was performed (Figure 3B). Solutions of the same fatty acids (50 and 500  $\mu$ M) and the L-R5 peptide (25–100  $\mu$ M) were incubated with Caco-2 cells for 24 hours. In contrast to the haemolysis test, no significant toxicity was revealed by this test.

The permeability and opening of TJs was also tested for these FAs in comparison to the L-R5 peptide (Figure 4A and 4B). The fatty acids as well as the peptide were incubated with Caco-2 cell layers for 3 hours after application to the apical side and the permeability of FD-4 was quantified. No significant increase in permeability was observed compared to HBSS control, with the exception of L-R5, which increased significantly the passage of FD-4 through the Caco-2 cell layers. The inability of fatty acids to increase permeability either by TJ modulation or toxic effects was further documented by the maintenance of the initial TEER value during incubation. However, the initial increase in permeability profile in the presence of FAs is different from that in the presence of L-R5.

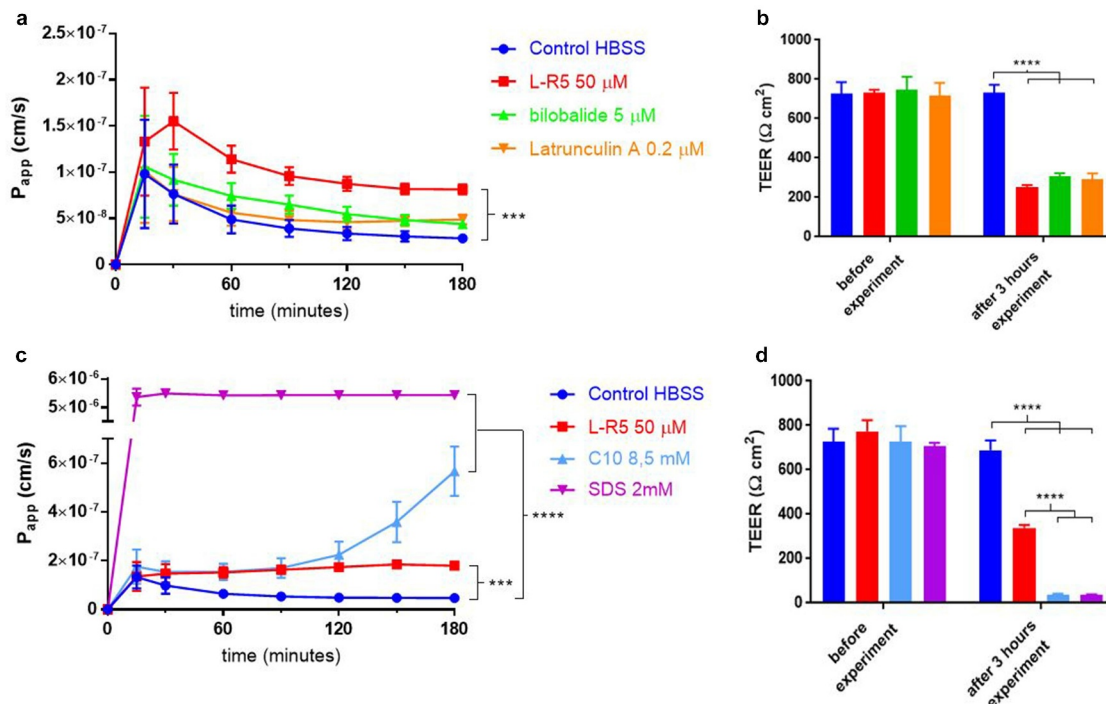


**Figure 2.** Comparison of permeability enhancement between L-R5 and other PEs. The permeability of FD-4 (0.25 mM solution) through Caco-2 epithelial cell layers was measured in the presence of L-R5 50  $\mu$ M, Bilobalide 5  $\mu$ M and Latrunculin A 0.2  $\mu$ M over 180 minutes (A). TEER was measured before and after the experiment (B). The permeability of FD-4 (0.25 mM solution) through Caco-2 epithelial cell layers was measured in the presence of L-R5 50  $\mu$ M, C<sub>10</sub> 8.5 mM and SDS 2 mM over 180 minutes (C). TEER was measured before and after the experiment (D). Values are mean  $\pm$  S.D. (n = 3), \*\*\**P* < 0.001, \*\*\*\**P* < 0.0001. The data were analysed using multiple t-test comparisons.



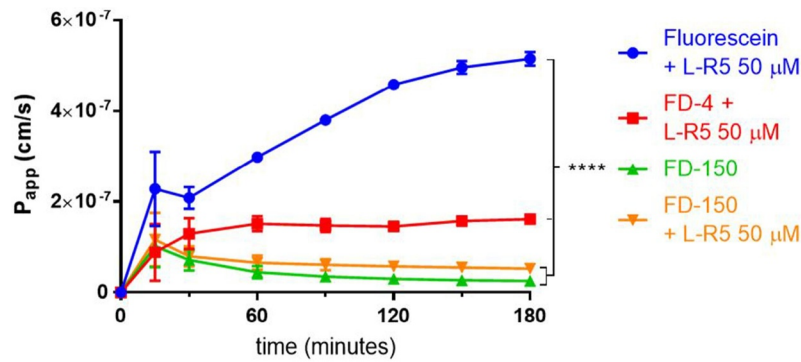


**Figure 5.** Size-dependent increase in permeability by L-R5. The permeability of sodium fluorescein, FD-4 and FD-150 (all 0.25 mM solution) through Caco-2 epithelial cell layers was measured in the presence of L-R5 (50 μM) over 180 minutes. Values are mean ± S.D. (n = 3), \*\*\*\**P* < 0.0001. The data were analyzed using multiple t-test comparisons.

significant difference to the control group. By contrast, the peptide without tryptophan (LW-5) still has an influence on the increase in FD-4 permeability. However, the effect is significantly lower than with L-R5.

The same peptide as L-R5 using D-amino acids (D-R5), as well as L-R5 with a scrambled sequence of amino acids (myr-WRARR) and ZIP were compared with respect to their effect on permeability and TEER in Caco-2 cell monolayers (Figure 7).

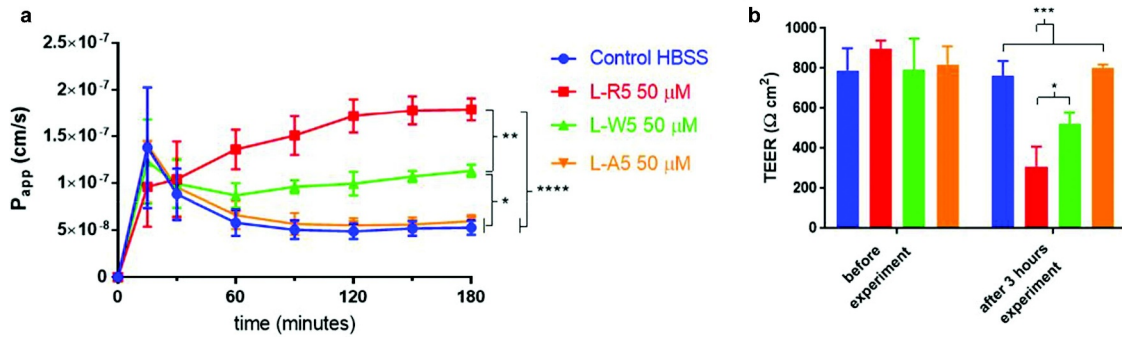


**Figure 6.** Permeability enhancement comparison between L-R5 and structural modifications of L-R5. The permeability of FD-4 (0.25 mM solution) through Caco-2 epithelial cell layers in the presence of L-R5, L-R5 with the tryptophan replaced by an alanine and L-R5 with the first arginine replaced by an alanine (all at a concentration of 50 μM) was investigated over 180 minutes (A). TEER was measured before and after the experiment (B). Values are mean ± S.D. (n = 3). \**P* < 0.05, \*\*\**P* < 0.001. The data were analysed using multiple t-test comparisons.

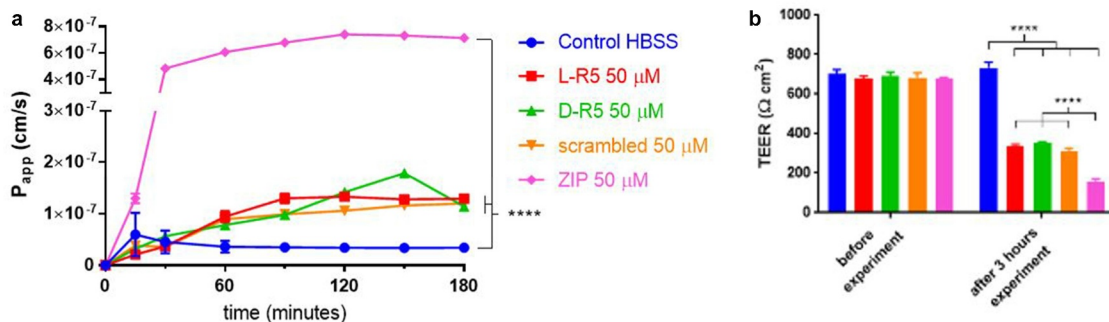


**Figure 7.** Permeability enhancement comparison between L-R5, its D form (D-R5), its scrambled form and ZIP. The permeability of FD-4 (0.25 mM solution) through Caco-2 epithelial cell layers was measured in the presence of L-R5, D-R5, scrambled L-R5 and ZIP (all at a concentration of 50 μM) over 180 minutes (A). TEER was measured before and after the experiment (B). Values are mean ± S.D. (n = 3). \*\*\*\**P* < 0.0001. The data were analysed using multiple t-test comparisons.

All 5-amino acid peptides, including the scrambled peptide, were shown to influence the permeability of FD-4 and the TEER of the cell layer in the same way, with FD-4 permeability increased and the TEER significantly decreased compared to the control group. Furthermore, the ZIP peptide increased the passage of FD-4 and decreased TEER to a higher extent than the other peptides.

#### 4. Discussion

The aim of this study was to investigate more deeply the ability of L-R5 to transiently open TJs. This opening seems to allow for the increase in permeation of molecules with a molecular weight < 150 kDa. Hemolytic and cytotoxicity tests were performed. In addition, a comparison with other PEs was carried out in order to attest the effect of L-R5. Finally, structural modifications of the peptide were applied to further elucidate the mechanism of action of the peptide.

L-R5 is more successful in increasing the permeability of FD-4 compared to the PEs bilobalide and latrunculin A (Figure 2A). The mechanisms of action of these two molecules are similar, as they both influence the cytoskeleton of the cell. By interacting with the adenosine A1 receptor, bilobalide causes contraction of the actin filament, which transiently opens intercellular junctions.<sup>41</sup> Latrunculin A enters the cell and disrupts the cytoskeletal filaments, distorting the cell and allowing larger molecules to pass through cellular junctions.<sup>42</sup> L-R5 has been designed to inhibit the activity of PKC  $\zeta$  in phosphorylating TJs proteins. Opening of TJs may be also due to influence of L-R5 cytoskeleton, as the enzyme was shown to be involved in cytoskeletal organization.<sup>31,45</sup> The opening induced by L-R5 appears to lead to a higher permeability with a faster onset, however, it should be noted that the applied concentrations of the other two molecules necessary to open TJs are much lower. An equivalent concentration of the peptide may give the same or even better results. The problem is that since latrunculin A is derived from a sponge toxin,<sup>46</sup> an increase in concentration may lead to safety issues. By contrast, bilobalide showed no cytotoxicity at a concentration of 625  $\mu$ M and may be more effective at higher

concentrations if no increase in toxicity is observed.<sup>41</sup> The fast increase in the first 15 minutes of each condition may be due to a hormetic effect,<sup>47</sup> even if this difference is not significant. More specifically, the modification of the ambient environment will inevitably force the cell to adapt. A greater disruption of the cell membrane by FAs is also a potential reason for this increase, which would lead to a short increase in paracellular permeability. Another explanation of this short greater permeation enhancement the formation of micelles between FD-4 and FAs.

L-R5 activity was also compared to C<sub>10</sub> and SDS (Figure 2C). SDS is supposed to increase transcellular permeability.<sup>48</sup> However, the concentration used here is toxic at 2 mM as reported in literature.<sup>44</sup> The increase in permeability is therefore probably due to cell death induced by this surfactant. TEER results for C<sub>10</sub> would suggest that it was also toxic at a concentration of 8.5 mM (Figure 2D). This molecule is thought to be responsible for a redistribution of TJ proteins.<sup>49</sup> The permeability profile shows that the increase in FD-4 passage is gradual. C<sub>10</sub> is therefore more effective than L-R5, but at a much higher concentration. Although no toxicity was demonstrated for C<sub>10</sub>,<sup>50,51</sup> administration of a reduced quantity may be beneficial for cellular health. On the other hand, a concentration of C<sub>10</sub> below its critical micellar concentration (CMC) has been shown to be more toxic due to medium chain fatty acid (MCFA) synthesis.<sup>52</sup> CMC may be pivotal for C<sub>10</sub> toxicity. For now, C<sub>10</sub> has been widely tested, above CMC at 8.5 mM, as a permeation enhancer in the absence of toxicity.

Although L-R5 has previously been shown not to cross epithelial cell layers, potentially avoiding systemic circulation,<sup>40</sup> the hemolytic effect of the peptide was tested (Figure 3A). Hemolysis occurs when the erythrocyte's cell membrane is disrupted. The haemolysis induced by L-R5 appears to be directly related to the fatty acid to which it is attached. The fatty acid moiety is necessary for its uptake into the cell. The larger the fatty acid, the greater the hemolytic effect. In addition, the unsaturated fatty acid induces hemolysis to a greater extent, which can be explained by a strong deformation of the cell membrane.<sup>53</sup> In view of these results, a reduction in the length of the fatty acid bound to L-R5 would

be desirable. However, this would result in a reduction of the penetrability of the peptide into the cell, and thus a reduction in the permeation effect, with the need to increase the dose administered. Increasing the peptide concentration does not appear to be toxic to the cell (Figure 3B). Furthermore, none of the fatty acids showed cytotoxicity in epithelial Caco-2 cell layers, even at high concentrations of up to 500  $\mu$ M. The hemolytic effect induced by the myristoyl tail would not have any consequence on *in vivo* application as we previously demonstrated that the peptide does not pass through the epithelial cell layer.<sup>40</sup>

It may be considered that the fatty acid is responsible for the increase in permeability, as it disrupts the membrane. However, as shown in Figure 4A, the passage of FD-4 in the presence of fatty acids through the Caco-2 cell layer remains similar to the control condition. Furthermore, TEER is not reduced by the fatty acids either (Figure 4B). All these results therefore confirm that L-R5 penetrates the cell by disrupting the cell membrane without being toxic and increases the permeability of FD-4 by a mechanism other than cell membrane disruption.

The permeability of FD-150 is only slightly increased by L-R5 (Figure 5). Very few non-specific paracellular PEs<sup>16</sup> were shown to increase the paracellular permeation of such large molecules, such as chitosan particles or liposomes.<sup>54,55</sup> 150 kDa therefore appears to be the limiting size for increased permeability induced by L-R5. However, an increase in peptide concentration may be sufficient to be more effective. 150 kDa is the average size of antibodies and therefore the largest treatments that can be prescribed.<sup>56</sup> The potential risk of pathogens and/or xenobiotics gaining access to subepithelial tissue through open TJs is a recurring concern in the discussion of permeation enhancers. We could show in this study that the upper size limit of substances permeating the disrupted tight junctions lies below a threshold of 150 kDa, which translates into a hydrodynamic radius of approximately 9 nm for dextran. This value is below the size of the majority of viral particles. In addition, as discussed in our recent paper,<sup>40</sup> the negative charge present at these junctions would additionally reduce the likelihood of viral permeation. Finally, TJ modulation by the peptide was demonstrated to be rapidly reversible.<sup>40</sup> The intestinal absorption of antibody formats or

large therapeutic proteins may be conceivable. Being able to formulate this type of treatment in a non-invasive dosage form would increase safety and reduce treatment costs. More *in vitro* and *in vivo* studies are needed to assess the suitability of using L-R5 in combination with a therapeutic drug.

Some structural modifications were applied to L-R5. It was shown that the presence of positive charges, conferred by arginine, is essential for the activity of the peptide (Figure 6A and 6B). In addition, the presence of a hydrophobic amino acid provides complementarity in the interaction, as the replacement of tryptophan by alanine significantly reduces the effect of the peptide. Further investigation on the correlation between peptide structure and its activity may lead to the development of more specific PKC  $\zeta$  competitors. As an example, phosphorylation of TJ protein occludin by PKC  $\zeta$  occurs at the C-terminal domain of the protein (between amino acids 403–438).<sup>57</sup> Specificity of the inhibition of this phosphorylation step may be achieved by adapting the sequence of small peptide inhibitors, possibly by increasing the number of positive charges. However, this would have to be weighed against a potential increase in toxicity caused by the higher cationic charge density of the compound.

The other peptides tested were D-R5, L-R5 with mixed amino acids (scrambled) and ZIP (Figure 7). D-R5 and scrambled peptides showed the same effect on FD-4 permeability as L-R5. The effect of D-R5 was expected, as it has the same sequence as L-R5. The use of D-R5 would be useful *in vivo* as a more metabolically stable form,<sup>58</sup> and a longer effect would potentially be visible due to its slower degradation. The effect of ZIP is stronger than for L-R5, which can be explained by its greater complementarity with the sequence of the target protein. ZIP has the same sequence as the PS and therefore the sequence that interacts with the protein *in vivo*. The advantage of using L-R5 instead of ZIP is found in the reduction of the time of action,<sup>40</sup> resulting in shorter disturbance of TJ integrity. The use of a peptide with a scrambled sequence compared to L-R5 resulted in a comparable activity, as was expected seen the nature of peptide–protein interaction.

The use of L-R5 as a PE can add value to a formulation for drug candidates of low bioavailability. Its effect is comparable to other PEs and no cytotoxicity has been revealed. Furthermore, the

opportunities for combination with drugs are wide given the possibility of increasing the paracellular permeation of molecules with a molecular weight of up to 150 kDa.

## 5. Conclusion

Modulation of TJs by interfering with PKC  $\zeta$  phosphorylation of TJ proteins has been shown to be suitable to increase epithelial permeability. The application of L-R5 peptide to intestinal cells *in vitro* is non-toxic and effective in transiently increasing the permeation of molecules with a suggested upper molecular weight limit of 150 kDa. Furthermore, the efficacy of permeation enhancement of the peptide is comparable to other PEs. Optimization of L-R5 in terms of target protein affinity and adaptation of activity kinetics appears to be possible by modification of the nature of the amino acids included. Finally, increase in activity through these modifications must be weighed against safety aspects.

## Acknowledgments

We would like to acknowledge the scientific advice and the revision received from Dr. Olivier Jordan, School of Pharmaceutical Sciences, University of Geneva.

## Disclosure statement

No potential conflict of interest was reported by the author(s).

## Funding

The author(s) reported there is no funding associated with the work featured in this article.

## References

- Alqahtani S. In silico ADME-Tox modeling: progress and prospects. *Expert Opin Drug Metab Toxicol.* 2017;13(11):1147–1158. doi:10.1080/17425255.2017.1389897.
- Savjani KT, Gajjar AK, Savjani JK. Drug solubility: importance and enhancement techniques. *ISRN Pharm.* 2012;2012:1–10. doi:10.5402/2012/195727.
- Lemmer HJ, Hamman JH. Paracellular drug absorption enhancement through tight junction modulation. *Expert Opin Drug Deliv.* 2013;10(1):103–114. doi:10.1517/17425247.2013.745509.
- Van Itallie CM, Holmes J, Bridges A, Gookin JL, Coccaro MR, Proctor W, Colegio OR, Anderson JM. The density of small tight junction pores varies among cell types and is increased by expression of claudin-2. *J Cell Sci.* 2008;121(3):298–305. doi:10.1242/jcs.021485.
- Van Itallie CM, Anderson JM. Architecture of tight junctions and principles of molecular composition. *Semin Cell Dev Biol.* 2014;36:157–165. doi:10.1016/j.semdb.2014.08.011.
- Luo X, Guo L, Zhang J, Xu Y, Gu W, Feng L, Wang Y. Tight junction protein occludin is a porcine epidemic diarrhea virus entry factor. *J Virol.* 2017;91(10). doi:10.1128/JVI.00202-17.
- Skamrahl M, Pang H, Ferle M, Gottwald J, Rübelling A, Maraspini R, Honigmann A, Oswald TA, Janshoff A. Tight junction ZO proteins maintain tissue fluidity. Ensuring Efficient Collective Cell Migration, *Adv Sci.* 2021:2100478. doi:10.1002/adv.202100478.
- Günzel D, Yu ASL. Claudins and the modulation of tight junction permeability. *Physiol Rev.* 2013;93(2):525–569. doi:10.1152/physrev.00019.2012.
- Kaminsky LW, Al-Sadi R, Ma TY. IL-1 $\beta$  and the intestinal epithelial tight junction barrier. *Front Immunol.* 2021;12:767456. doi:10.3389/fimmu.2021.767456.
- Al-Sadi R. Mechanism of cytokine modulation of epithelial tight junction barrier. *Front Biosci.* 2009:2765. doi:10.2741/3413.
- Shin K, Fogg VC, Margolis B. Tight Junctions and Cell Polarity, *Annu. Rev Cell Dev Biol.* 2006;22(1):207–235. doi:10.1146/annurev.cellbio.22.010305.104219.
- O’Leary LF, Tomko AM, Dupré DJ. Polarity scaffolds signaling in epithelial cell permeability. *Inflamm Res.* 2021;70(5):525–538. doi:10.1007/s00011-021-01454-1.
- Leonardo TR, Shi J, Chen D, Trivedi HM, Chen L. Differential expression and function of bicellular tight junctions in skin and oral wound healing. *IJMS.* 2020;21(8):2966. doi:10.3390/ijms21082966.
- Stuart RO, Nigam SK. Regulated assembly of tight junctions by protein kinase C. *Proc Nat Acad Sci.* 1995;92: 6072–6076. doi: 10.1073/pnas.92.13.6072.
- Ogasawara N, Kojima T, Go M, Ohkuni T, Koizumi J, Kamekura R, Masaki T, Murata M, Tanaka S, Fuchimoto J, et al. PPAR $\gamma$  agonists upregulate the barrier function of tight junctions via a PKC pathway in human nasal epithelial cells. *Pharmacol Res.* 2010;61(6):489–498. doi:10.1016/j.phrs.2010.03.002.
- Brunner J, Ragupathy S, Borchard G. Target specific tight junction modulators. *Adv Drug Deliv Rev.* 2021;171:266–288. doi:10.1016/j.addr.2021.02.008.
- Twarog C, Fattah S, Heade J, Maher S, Fattal E, Brayden DJ. Intestinal permeation enhancers for oral delivery of macromolecules: a comparison between salcaprozate sodium (SNAC) and sodium caprate (C10. *Pharmaceutics.* 2019;11(2):78. doi:10.3390/pharmaceutics11020078.

18. Liang W, Xu W, Zhu J, Zhu Y, Gu Q, Li Y, Guo C, Huang Y, Yu J, Wang W, et al. Ginkgo biloba extract improves brain uptake of ginsenosides by increasing blood-brain barrier permeability via activating A1 adenosine receptor signaling pathway. *J Ethnopharmacol.* **2020**;246:112243. doi:10.1016/j.jep.2019.112243.
19. Shiobara T, Usui T, Han J, Isoda H, Nagumo Y. The reversible increase in tight junction permeability induced by capsaicin is mediated via cofilin-actin cytoskeletal dynamics and decreased level of occludin. *PLoS ONE.* **2013**;8(11):e79954. doi:10.1371/journal.pone.0079954.
20. Danielsen EM, Hansen GH. Probing paracellular -versus transcellular tissue barrier permeability using a gut mucosal explant culture system. *Tissue Barriers.* **2019**;7(1):1601955. doi:10.1080/21688370.2019.1601955.
21. Cario E, Gerken G, Podolsky DK. Toll-like receptor 2 enhances ZO-1-associated intestinal epithelial barrier integrity via protein kinase C. *Gastroenterology.* **2004**;127(1):224–238. doi:10.1053/j.gastro.2004.04.015.
22. Li Z, Liu X, Liu Y, Xue Y, Wang P, Liu L, Liu J, Yao Y, Ma J. Roles of serine/threonine phosphatases in low-dose endothelial monocyte-activating polypeptide-II-induced opening of blood–tumor barrier. *J Mol Neurosci.* **2015**;57(1):11–20. doi:10.1007/s12031-015-0604-8.
23. Hug H, Sarre TF. Protein kinase C isoenzymes: divergence in signal transduction? *Biochem J.* **1993**;291(2):329–343. doi:10.1042/bj2910329.
24. Goldstein B, Macara IG. The PAR proteins: fundamental players in animal cell polarization. *Dev Cell.* **2007**;13(5):609–622. doi:10.1016/j.devcel.2007.10.007.
25. Sakane F, Hoshino F, Ebina M, Sakai H, Takahashi D. The roles of diacylglycerol kinase  $\alpha$  in cancer cell proliferation and apoptosis. *Cancers.* **2021**;13(20):5190. doi:10.3390/cancers13205190.
26. Nusrat A, Turner JR, Madara JL. Molecular physiology and pathophysiology of tight junctions. IV. Regulation of tight junctions by extracellular stimuli: nutrients, cytokines, and immune cells. *Am J Physiol Gastrointest Liver Physiol.* **2000**;279(5):G851–857. doi:10.1152/ajpgi.2000.279.5.G851.
27. Dempsey EC, Newton AC, Mochly-Rosen D, Fields AP, Reyland ME, Insel PA, Messing RO. Protein kinase C isozymes and the regulation of diverse cell responses. *Am J Physiol Lung Cell Mol Physiol.* **2000**;279(3):L429–L438. doi:10.1152/ajplung.2000.279.3.L429.
28. Sadeghi MM, Salama MF, Hannun YA. Protein kinase C as a therapeutic target in non-small cell lung cancer. *IJMS.* **2021**;22(11):5527. doi:10.3390/ijms22115527.
29. Apostolatos A, Song S, Acosta S, Peart M, Watson JE, Bickford P, Cooper DR, Patel NA. Insulin promotes neuronal survival via the alternatively spliced protein kinase C $\delta$ II isoform. *J Biol Chem.* **2012**;287(12):9299–9310. doi:10.1074/jbc.M111.313080.
30. Fields AP, Murray NR. Protein kinase C isozymes as therapeutic targets for treatment of human cancers. *Adv Enzyme Regul.* **2008**;48(1):166–178. doi:10.1016/j.advenzreg.2007.11.014.
31. Ratnayake WS, Apostolatos CA, Breedy S, Dennison CL, Hill R, Acevedo-Duncan M. Atypical PKCs activate Vimentin to facilitate prostate cancer cell motility and invasion. *Cell Adh Migr.* **2021**;15(1):37–57. doi:10.1080/19336918.2021.1882782.
32. Manda B, Mir H, Gangwar R, Meena AS, Amin S, Shukla PK, Dalal K, Suzuki T, Rao RK. Phosphorylation hotspot in the C-terminal domain of occludin regulates the dynamics of epithelial junctional complexes. *J Cell Sci.* **2018**;jcs.206789. doi:10.1242/jcs.206789.
33. Stevenson BR, Anderson JM, Braun ID, Mooseker MS. Phosphorylation of the tight-junction protein ZO-1 in two strains of Madin-Darby canine kidney cells which differ in transepithelial resistance. *Biochem J.* **1989**;263(2):597–599. doi:10.1042/bj2630597.
34. Tsai L-CL, Xie L, Dore K, Xie L, Del Rio JC, King CC, Martinez-Ariza G, Hulme C, Malinow R, Bourne PE, et al. Zeta inhibitory peptide disrupts electrostatic interactions that maintain atypical protein kinase C in its active conformation on the scaffold p62. *J Biol Chem.* **2015**;290(36):21845–21856. doi:10.1074/jbc.M115.676221.
35. Laudanna C, Mochly-Rosen D, Constantin G, Butcher EC, Liron T. Evidence of  $\zeta$  protein kinase C involvement in polymorphonuclear neutrophil integrin-dependent adhesion and chemotaxis. *J Biol Chem.* **1998**;273(46):30306–30315. doi:10.1074/jbc.273.46.30306.
36. Steinberg SF. Structural basis of protein kinase C isoform function. *Physiol Rev.* **2008**;88(4):1341–1378. doi:10.1152/physrev.00034.2007.
37. Wu-Zhang AX, Schramm CL, Nabavi S, Malinow R, Newton AC. Cellular pharmacology of protein kinase M $\zeta$  (PKM $\zeta$ ) contrasts with its in vitro profile. *J Biol Chem.* **2012**;287(16):12879–12885. doi:10.1074/jbc.M112.357244.
38. Brunner J, Schwartz D, Hainard A, Gouiller A, Borchard G. Impact of L-R5 permeation enhancer on TJs opening cellular mechanisms. **2022**. Unpublished Paper.
39. Ragupathy S, Esmaili F, Paschoud S, Sublet E, Citi S, Borchard G. Toll-like receptor 2 regulates the barrier function of human bronchial epithelial monolayers through atypical protein kinase C zeta, and an increase in expression of claudin-1. *Tissue Barriers.* **2014**;2:e29166. doi:10.4161/tisb.29166.
40. Ragupathy S, Brunner J, Borchard G. Short peptide sequence enhances epithelial permeability through interaction with protein kinase C. *Eur J Pharm Sci.* **2021**;160:105747. doi:10.1016/j.ejps.2021.105747.
41. Guo C, Wang H, Liang W, Xu W, Li Y, Song L, Zhang D, Hu Y, Han B, Wang W, et al. Bilobalide reversibly modulates blood-brain barrier permeability through promoting adenosine A1 receptor-mediated phosphorylation of actin-binding proteins. *Biochem Biophys Res Commun.* **2020**;526(4):1077–1084. doi:10.1016/j.bbrc.2020.03.186.

42. Song H, Zhang J, He W, Wang P, Wang F. Activation of cofilin increases intestinal permeability via depolymerization of F-Actin during hypoxia in vitro. *Front Physiol.* 2019;10:1455. doi:10.3389/fphys.2019.01455.
43. Maher M, Illum. Transmucosal absorption enhancers in the drug delivery field. *Pharmaceutics.* 2019;11(7):339. doi:10.3390/pharmaceutics11070339.
44. Welch J, Wallace J, Lansley AB, Roper C. Evaluation of the toxicity of sodium dodecyl sulphate (SDS) in the MucilAir<sup>TM</sup> human airway model in vitro. *Regul Toxicol Pharmacol.* 2021;125:105022. doi:10.1016/j.yrtph.2021.105022.
45. Guo H, Gu F, Li W, Zhang B, Niu R, Fu L, Zhang N, Ma Y. Reduction of protein kinase C  $\zeta$  inhibits migration and invasion of human glioblastoma cells. *J Neurochem.* 2009;109(1):203–213. doi:10.1111/j.1471-4159.2009.05946.x.
46. Cheney KL, White A, Mudianta IW, Winters AE, Quezada M, Capon RJ, Mollo E, Garson MJ. Choose your weaponry: selective storage of a single toxic compound, latrunculin A, by closely related nudibranch molluscs. *PLoS ONE.* 2016;11(1):e0145134. doi:10.1371/journal.pone.0145134.
47. Marchant GE. Hormesis and toxic torts. *Hum Exp Toxicol.* 2008;27(2):97–107. doi:10.1177/0960327107086567.
48. Maher S, Mrsny RJ, Brayden DJ. Intestinal permeation enhancers for oral peptide delivery. *Adv Drug Deliv Rev.* 2016;106(Pt B):277–319. doi:10.1016/j.addr.2016.06.005.
49. Maher S, Leonard TW, Jacobsen J, Brayden DJ. Safety and efficacy of sodium caprate in promoting oral drug absorption: from in vitro to the clinic. *Adv Drug Deliv Rev.* 2009;61(15):1427–1449. doi:10.1016/j.addr.2009.09.006.
50. Twarog C, Liu K, O'Brien PJ, Dawson KA, Fattal E, Illel B, Brayden DJ. A head-to-head Caco-2 assay comparison of the mechanisms of action of the intestinal permeation enhancers: SNAC and sodium caprate (C10). *Eur J Pharm Biopharm.* 2020;152:95–107. doi:10.1016/j.ejpb.2020.04.023.
51. Raoof AA, Chiu P, Ramtoola Z, Cumming IK, Teng C, Weinbach SP, Hardee GE, Levin AA, Geary RS. Oral bioavailability and multiple dose tolerability of an anti-sense oligonucleotide tablet formulated with sodium caprate. *J Pharm Sci.* 2004;93(6):1431–1439. doi:10.1002/jps.20051.
52. Borrull A, López-Martínez G, Poblet M, Cordero-Otero R, Rozès N. New insights into the toxicity mechanism of octanoic and decanoic acids on *Saccharomyces cerevisiae*. *Yeast.* 2015;32(5):451–460. doi:10.1002/yea.3071.
53. Løvstad RA. Fatty acid induced hemolysis. protective action of ceruloplasmin, albumins, thiols and vitamin C. *Int J Biochem.* 1986;18(9):771–775. doi:10.1016/0020-711X(86)90052-2.
54. Gradauer K, Dünnhaupt S, Vonach C, Szöllösi H, Pali-Schöll I, Mangge H, Jensen-Jarolim E, Bernkop-Schnürch A, Prassl R. Thiomers-coated liposomes harbor permeation enhancing and efflux pump inhibitory properties. *J Control Release.* 2013;165(3):207–215. doi:10.1016/j.jconrel.2012.12.001.
55. Hombach J, Bernkop-Schnürch A. Chitosan solutions and particles: evaluation of their permeation enhancing potential on MDCK cells used as blood brain barrier model. *Int J Pharm.* 2009;376(1–2):104–109. doi:10.1016/j.ijpharm.2009.04.027.
56. Ma H, O'Kennedy R. The structure of natural and recombinant antibodies. In: Houen G, editor. *Peptide Antibodies*. New York, New York, NY: Springer; 2015. p. 7–11. doi:10.1007/978-1-4939-2999-3\_2.
57. Jain S, Suzuki T, Seth A, Samak G, Rao R. Protein kinase C $\zeta$  phosphorylates occludin and promotes assembly of epithelial tight junctions. *Biochem J.* 2011;437(2):289–299. doi:10.1042/BJ20110587.
58. Verdurmen WPR, Bovee-Geurts PH, Wadhvani P, Ulrich AS, Hällbrink M, van Kuppevelt TH, Brock R. Preferential uptake of L- versus D-Amino acid cell-penetrating peptides in a cell type-dependent manner. *Chem Biol.* 2011;18:1000–1010. doi:10.1016/j.chembiol.2011.06.006.